ESC European Society of Cardiology

European Heart Journal - Cardiovascular Imaging (2026) **27**, 400–412
https://doi.org/10.1093/ehjci/jeaf297

ORIGINAL PAPER

Scar architecture as a structural biomarker of ventricular arrhythmias and sudden cardiac death in patients with hypertrophic cardiomyopathy: a cardiac magnetic resonance study

Pietro Francia [1], Giulio Falasconi [2], Maria Beatrice Musumeci[1], Elena Biagini [3,4], Pedro Freitas[5], Diego Penela [6], José Tomás Ortiz-Pérez[7,8], Giacomo Tini[1], Matteo Sclafani[1,9], Maria Alessandra Schiavo[3,4], Rita Amador [5], Sebastiano Carli[6], Guido del Monaco[6], Cristina Panico [6], David Soto-Iglesias [2], Paula Franco-Ocaña [2], Raffaello Ditaranto[3,4], Andrea Saglietto [10,11], Julio Martì-Almor[2], Camillo Autore[12], and Antonio Berruezo [2]*

[1]Department of Clinical and Molecular Medicine, Cardiology Unit, Sant'Andrea University Hospital, University Sapienza, Rome, Italy; [2]Arrhythmia Department, Teknon Heart Institute, Teknon Medical Center, Calle Villana 12 (08022), Barcelona, Spain; [3]European Reference Network for Rare, Low Prevalence and Complex Diseases of the Heart-ERN GUARD-Heart, Bologna, Italy; [4]Cardiac Thoracic and Vascular Department, Cardiology Unit, IRCCS Azienda Ospedaliero-Universitaria di Bologna, Bologna, Italy; [5]Cardiology Department, Hospital Santa Cruz, Centro Hospitalar Lisboa Ocidental, Lisbon, Portugal; [6]IRCCS Humanitas Research Hospital, Department of Biomedical Sciences, Humanitas University, Rozzano, Italy; [7]Institut D'Investigacions Biomèdiques August Pi I Sunyer (IDIBAPS), Barcelona, Spain; [8]Acute Cardiac Care Section, Cardiovascular Institute, Hospital Clínic, Barcelona, Spain; [9]Royal Brompton and Harefield Hospitals, Guy's and St Thomas' NHS Foundation Trust, London, UK; [10]Division of Cardiology, Cardiovascular and Thoracic Department, 'Citta Della Salute e Della Scienza' Hospital, Turin, Italy; [11]Department of Medical Sciences, University of Turin, Turin, Italy; and [12]Department of Cardiovascular and Respiratory Sciences, San Raffaele, Cassino, FR, Italy

Received 14 August 2025; revised 10 October 2025; accepted 21 October 2025; online publish-ahead-of-print 28 October 2025

See the editorial comment for this article 'Scar architecture in hypertrophic cardiomyopathy—the geometry of fate', by P. Bhagirath and I. Roca-Luque, https://doi.org/10.1093/ehjci/jeaf326.

Aims Myocardial scarring assessed by late gadolinium enhancement cardiac magnetic resonance (LGE-CMR) predicts sudden cardiac death (SCD) in hypertrophic cardiomyopathy (HCM). Post-processing enables characterization of scar components: borderzone (BZ), core, and BZ channels.

Methods and results Evaluate scar composition as a predictor of VT/VF beyond traditional risk factors in HCM. We retrospectively analyzed HCM patients who underwent LGE-CMR. Scar components, alone or combined with ESC or ACC/AHA risk scores, were tested as predictors of a composite VT/VF endpoint (SCD, sustained VT, ICD therapy, or cardiac arrest). Four-hundred-ten patients (67% males, 55 years IQR: 41–65) were included, 298 of whom (72.6%) had LGE at CMR (LGE+). Total scar, BZ and core mass were 7.3% (IQR: 0.0–14.3), 6.4% (IQR: 0.0–12.2), and 0.9% (IQR: 0.0–2.1) of LV mass, respectively. BZ channels were found in 140 (34.1%) patients. At follow-up (65 months; IQR: 36–95), 26 (6.3%) patients met the endpoint. Total scar, BZ and core mass were higher in VT/VF patients ($P < 0.001$). BZ channels were observed in 88.5% of VT/VF patients vs. 30.5% of those without ($P < 0.001$). Patients with BZ channels had higher incidence of VT/VF. BZ channels mass was associated with an increased risk of VT/VF after adjustment for ESC (HR: 1.45; 95% CI: 1.26–1.67; $P < 0.0001$) and AHA/ACC (HR: 1.34; 95% CI: 1.16–1.54; $P < 0.0001$) risk estimate. The predictive performance of both ESC and AHA/ACC models was enhanced by integrating BZ channel mass (NRI: 0.19, $P = 0.03$ and 0.32, $P < 0.001$, respectively).

* Corresponding author. E-mail: antonio.berruezo@quironsalud.es

Conclusion Scar composition and its organization in BZ channels provides strong, independent prognostic value for VT/VF in HCM, improving existing clinical risk stratification tools.

Graphical Abstract

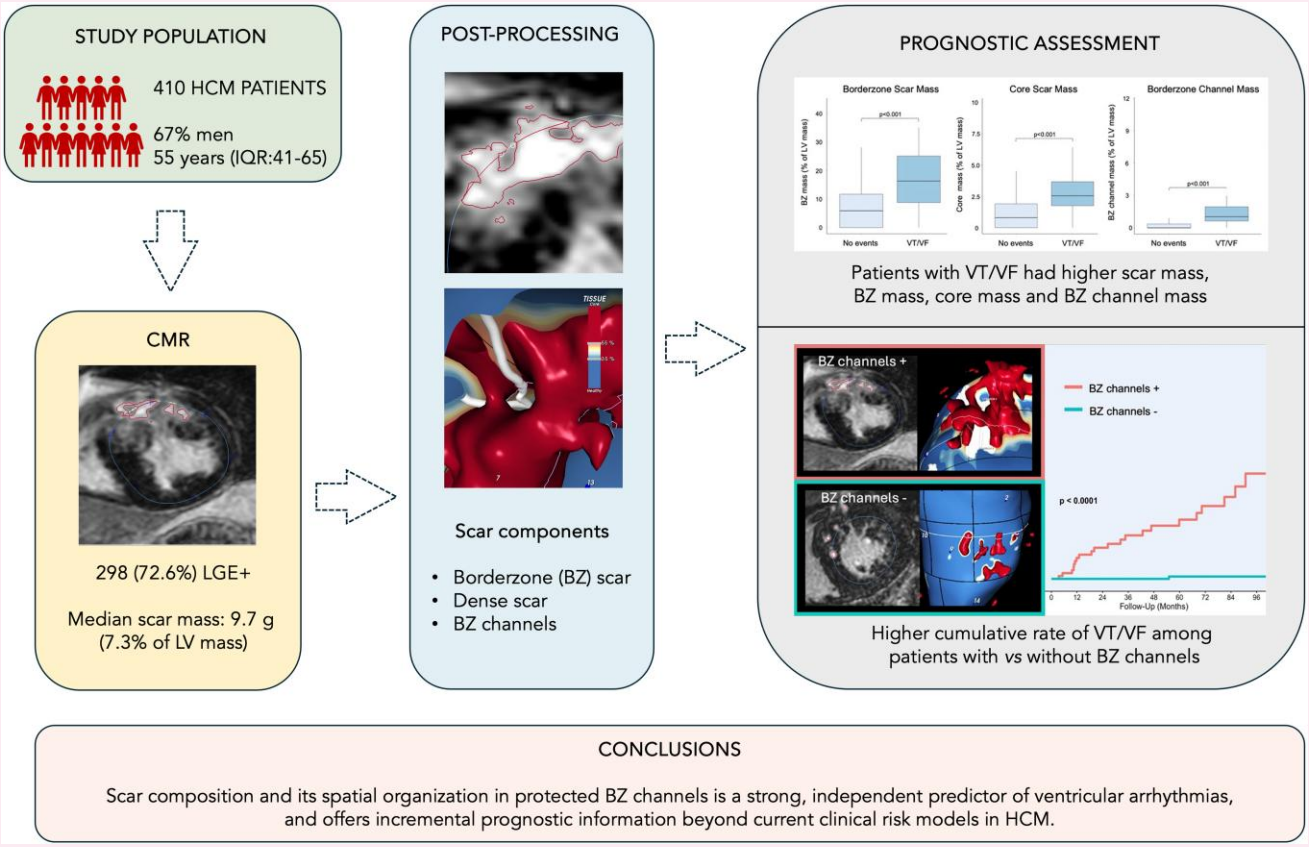

Keywords hypertrophic cardiomyopathy • late gadolinium enhancement • scar • cardiac magnetic resonance • sudden cardiac death

Background

Myocardial scar, identified by cardiac magnetic resonance with late gadolinium enhancement (LGE-CMR), is common in hypertrophic cardiomyopathy (HCM).[1,2] Studies show that HCM patients with LGE have higher risk of ventricular arrhythmias (VA) and sudden cardiac death (SCD).[2–6] In particular, extensive LGE (≥15% LV myocardium) is an independent SCD predictor,[3] and guidelines include it as a risk factor.[7,8] However, it has been reported that not only the amount, but also characteristics and three-dimensional distribution of LGE affect the risk of VA in HCM. Indeed, non-homogeneous scar patterns as assessed by LGE-dispersion mapping,[9] scar entropy[5] and myocardial LGE radiomics[10] add prognostic value beyond scar mass, though mechanisms remain unclear.

Post-processing of LGE-CMR images allow for the characterization of dense fibrosis (scar core), diffuse fibrosis (border zone, BZ), and BZ channels—strands of BZ tissue embedded within unexcitable scar (core) that connect regions of healthy myocardium.[11,12] These protected channels are a part of reentry circuits[13] and predict appropriate ICD therapies in high-risk HCM patients.[14] However, it is unknown if scar composition and BZ channels refine VA risk in unselected HCM.

We assessed a large population of unselected HCM patients to (a) describe LGE prevalence and scar composition; (b) link scar patterns with clinical phenotypes; (c) assess scar architecture as a predictor of VA and SCD beyond traditional risk factors; (d) evaluate if scar characteristics improve European Society of Cardiology (ESC) and American Heart Association/American College of Cardiology (AHA/ACC) risk models.

Methods

Study population

We retrospectively analyzed a prospectively followed cohort of HCM patients who underwent LGE-CMR at five centres (Sant'Andrea University Hospital, IT; IRCCS University Hospital of Bologna, IT; Hospital Santa Cruz, PRT; IRCCS Humanitas Research Hospital, IT; Teknon Medical Center, ES) between May 2006 and October 2023.

Exclusion criteria were CMR scans without intravenous gadolinium contrast agent, unavailable or corrupted original digital CMR files, and poor-quality CMR exams preventing accurate post-processing. As the subtle rim of fibrosis post-septal reduction interventions in obstructive HCM

patients can alter the architecture of disease-related myocardial scar, patients who underwent myectomy or septal alcohol ablation after CMR were also excluded.

The diagnosis of HCM was based on echocardiographic demonstration of a hypertrophied and non-dilated left ventricle in the absence of any other cardiac or systemic disease that could result into a comparable LV hypertrophy.[15,16] Patients with metabolic/infiltrative diseases were excluded. LV outflow tract obstruction was defined as a peak instantaneous gradient ≥30 mmHg on Doppler echocardiography, at rest or after provocation. HCM with systolic LV dysfunction was defined as LV ejection fraction <50%.

Patients were referred for ICD implantation according to the ESC or AHA/ACC guidelines available at the time of defibrillator candidacy, generally when presenting one or more established risk factors for SCD.[16] As from 2014, shared decision making for ICD implantation was also supported by the 5-year SCD risk score endorsed by the ESC.[15] The study was approved by the local Ethical Committee of the participating centres and signed informed consent was provided. The data that support the findings of this study are available from the corresponding author upon reasonable request.

CMR imaging and processing

CMRs were performed with 1.5-T scanners (Philips, GE Medical Systems, or Siemens) and analyzed locally. LGE was acquired 10–20 min after 0.1–0.2 mmol/kg i.v. gadolinium with breath-hold segmented gradient-echo inversion-recovery or PSIR sequences. LGE was acquired 10–20 min after 0.1–0.2 mmol/kg i.v. gadolinium with segmented gradient-echo inversion-recovery or PSIR sequences. For analysis, only magnitude (MAG) images were used, ensuring methodological homogeneity across the study population irrespective of the acquisition sequence. Inversion time was optimized to null normal myocardium. Most exams were 2D (92.0%). The mean slice thickness was 8.5 ± 1.2 mm.

Post-processing of LGE images was centralized in core lab with ADAS 3D (Galgo Medical, Barcelona, Spain) according to a previously described protocol.[17] Briefly, the LV was reconstructed in axial view and divided into 9 concentric 3D shells from endocardium to epicardium (10–90% wall thickness: endocardial = 10–20%, mid-myocardial = 30–70%, epicardial = 80–90%). LV subendocardial (10%) and subepicardial (90%) layers were used instead of the true endocardial and epicardial shells to avoid the partial volume effect.[18] Color-coded pixel signal intensity (PSI) maps based on LGE-CMR images were projected to each shell. LGE mass was calculated using the full-width half-maximum method. If no fibrosis was visually detected, LGE measures were set to zero. A PSI-based algorithm classified tissue as scar core, BZ, or healthy (thresholds 40 ± 5% and 60 ± 5%), as previously described.[18] The total scar mass, BZ mass, and core mass in each shell were automatically measured using ADAS 3D LV. BZ channels, defined as continuous corridors of BZ surrounded by scar core or an anatomical barrier (e.g. mitral annulus) connecting two areas of healthy tissue, were automatically identified (*Figure 1*). BZ channel mass (grams of BZ tissue that make up all the channels) was obtained by multiplying the number of image voxels within the identified channel by the voxel volume and a myocardial density of 1.05 g/cm^3, using a full-automated tool. A good intra- and inter-observer agreement for this technique has already been reported.[17] Analysis of LGE-CMRs was conducted by two cardiologists with specific expertise in cardiac imaging post-processing. (P.F. and G.F.) and one senior cardiologist with more than 15 years of experience in CMR (J.T.O.P.) that were blinded to clinical and follow-up data.

End-points and follow-up

The study endpoint of ventricular tachycardia or fibrillation (VT/VF) was defined as the occurrence of SCD, resuscitated cardiac arrest, sustained VT, or appropriate ICD therapies for VT or VF. All events, including stored intracardiac electrograms of ICD interventions, were reviewed and adjudicated at each centre. Follow-up was from the date of CMR to the last follow-up visit or device interrogation, death or heart transplantation.

Risk prediction analysis

SCD risk was estimated using ESC[7] and ACC/AHA[8] models. To account for the expected limited number of SCD events, hazard ratios were adjusted only for a predefined 'high risk condition' covariate—class I or IIa ICD indication per ESC (Model 1) and AHA/ACC (Model 2)—rather than for each risk factor.[10] As per ESC guidelines for the prevention of SCD,[7] this condition includes patients with >6% 5-year risk of SCD or ≥4% to 6% when associated with additional risk markers (LGE ≥15% of LV mass, EF <50%, apical aneurysm). Children <16 years were assessed by the HCM Risk-Kids score[19] and deemed high risk if the estimated 5-year risk was ≥6%. As per AHA/ACC guidelines,[8] the high risk condition included adults with at least 1 major risk factor for SCD among (a) familial history of SCD in a first-degree relative <50 years, (b) massive LVH (≥30 mm in any LV segment), (c) unexplained syncope, (d) apical aneurysm, (e) EF <50%. Children with at least 1 risk factor were considered high risk.

Secondary prevention ICD recipients were considered high risk in both models. All scores were calculated at the index CMR.

Statistical analysis

Continuous variables are given as mean ± standard deviation for normally distributed data or median (interquartile range, IQR) in case of skewed distribution. Categorical variables are given as absolute numbers and percentages. To compare two variables, the Student's *t*-test or Wilcoxon test were used. Proportions were compared using the chi-square test.

Cox proportional hazard models were used to assess relative risks. The binary variable 'high risk condition' according to the ESC[7] and AHA/ACC[8] models was entered into the two multivariate cause-specific hazards models to estimate the independent effect of the scar characteristics on the occurrence of VT/VF. Receiver operating characteristic (ROC) analysis was used to calculate the sensitivity, specificity, and AUC of the scar characteristics as well as the incremental prognostic value of adding LGE features to current risk models. We used categorical net reclassification analysis to assess the improvement in VT/VF risk prediction achieved by incorporating BZ channels mass into the ESC or ACC/AHA models (i.e. net reclassification improvement, NRI). The integrated model was developed using the predicted probabilities from a logistic regression including the two covariates. The reclassification matrices were constructed using an optimized cut-off threshold for the predicted probabilities, determined by the Youden index, to define two categories (low risk and high risk). Kaplan–Meier curves and the log-rank test were used to assess the cumulative incidence of the combined primary endpoint of VT/VF according to different scar characteristics.

All tests were two-sided, and a P value of < 0.05 was considered statistically significant. Statistical analysis was performed using R version 3.6.2 software (R Foundation for Statistical Computing, Vienna, Austria).

Results

Study population

We evaluated 436 patients. Of these, 20 underwent septal reduction after CMR and were excluded, and 6 were lost to follow-up. Therefore, the final study group comprised 410 patients. The mean age at first CMR was 52 ± 17 years. Baseline clinical characteristics are presented in *Table 1*.

CMR imaging and scar architecture

LGE was detected in 298 (72.6%) patients. The LV regions most frequently involved according to the AHA 17 segments model were the mid anterior and anteroseptal ones (segments 7 and 8; 37% and 33%

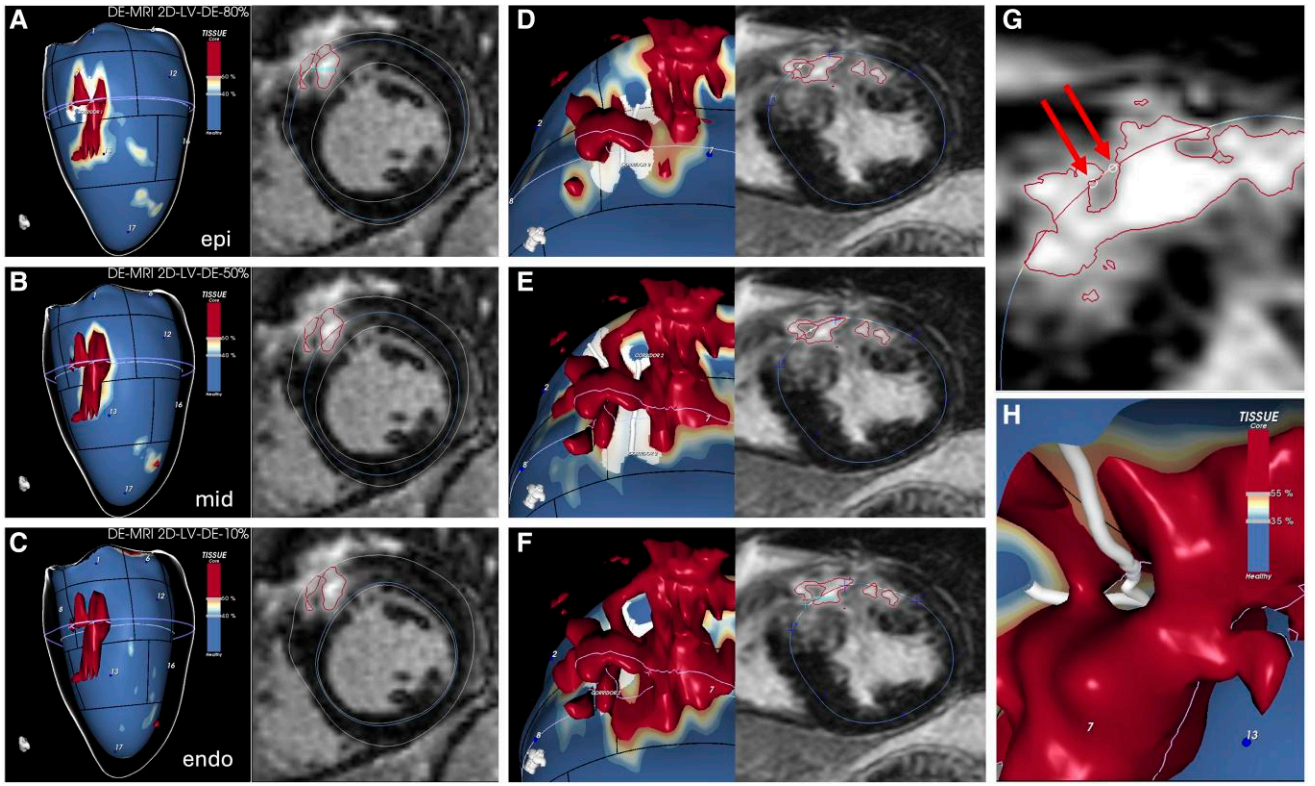

Figure 1 Post-processing of LGE-CMRs. (*A–C*): short axis view and 3D color-coded LV reconstruction showing mid/anterior-apical scar (AHA segments 7 and 13). From top to bottom, layers (epicardial, mid, endocardial) are color-coded: dense scar = red, BZ = yellow/orange, healthy = blue. An epicardial BZ channel appears as a white channel between healthy myocardium and dense scar. (*D–F*): large and heterogeneous LV scar in a patient with massive LV hypertrophy. 3D view of the scar shows a BZ channel embedded within dense scar at 80%, 70%, and 60% wall thickness. (*G* and *H*): the CMR slice just basal to the previous one (70% layer) shows a channel bifurcation (arrows in G), and 3D view from the inner layer (H).

Table 1 Comparison of baseline clinical characteristics of HCM patients with and without VT/VF at follow-up

Characteristics	All ($n = 410$)	VT/VF − ($n = 384$)	VT/VF + ($n = 26$)	P
Male sex, *n* (%)	273 (66.6%)	253 (65.9%)	20 (76.9%)	0.289
Age at CMR (years)	55.0 (41.0, 64.8)	55.0 (42.0, 65.0)	50.0 (36.0, 59.0)	0.177
Clinical				
LVOT gradient ≥30 mm Hg	81 (19.8%)	78 (20.3%)	3 (11.5%)	0.443
Atrial fibrillation, *n* (%)	64 (15.6%)	55 (14.3%)	9 (34.6%)	0.011
Beta-blockers, *n* (%)	273 (66.6%)	251 (65.4%)	22 (84.6%)	0.052
Risk factors				
Unexplained syncope, *n* (%)	33 (8.0%)	30 (7.8%)	3 (11.5%)	0.454
Family history of SCD, *n* (%)	65 (15.9%)	58 (15.1%)	7 (26.9%)	0.159
Max wall thickness (mm)	18.0 (16.0, 22.0)	18.0 (16.0, 22.0)	20.5 (19.0, 27.0)	0.003
Max wall thickness >30 mm, *n* (%)	46 (11.2%)	39 (10.1%)	7 (26.9%)	0.014
NSVT, *n* (%)	123 (30.0%)	107 (27.9%)	16 (61.5%)	<0.001
Apical aneurysm, *n* (%)	15 (3.7%)	12 (3.1%)	3 (11.5%)	0.062
EF <50%, *n* (%)	26 (6.3%)	19 (4.9%)	7 (26.9%)	<0.001
ESC 5-years risk of SD (%)	2.4 (1.6, 4.4)	2.3 (1.6, 4.1)	4.6 (3.3, 5.9)	<0.001

LVOT, left ventricular outflow tract; NSVT, non-sustained ventricular tachycardia; SCD, sudden cardiac death.

Table 2 Scar characteristics of HCM patients with and without VT/VF during follow-up

Characteristics	All ($n = 410$)	VT/VF − ($n = 384$)	VT/VF + ($n = 26$)	P
LV mass, g	137.6 (105.3, 177.3)	134.1 (104.4, 170.7)	190.9 (163.2, 228.0)	<0.001
LV mass index (g/m^2)	73.0 (56.7, 92.0)	71.6 (56.4, 89.2)	97.0 (82.3, 127.5)	0.003
LGE + patients, *n* (%)	298 (72.7%)	273 (71.1%)	25 (96.2%)	<0.001
Scar mass, g	9.7 (0.0, 22.3)	8.6 (0.0, 20.5)	38.0 (21.9, 59.1)	<0.001
Scar/LV mass ratio (%)	7.3 (0.0, 14.3)	7.0 (0.0, 13.5)	19.7 (10.2, 30.5)	<0.001
Scar >15% of LV mass, *n* (%)	97 (23.7)	82 (21.3)	15 (57.7)	<0.001
BZ mass, g	8.0 (0.0, 19.2)	7.6 (0.0, 16.7)	27.3 (16.0, 49.3)	<0.001
BZ/LV mass ratio (%)	6.4 (0.0, 12.2)	5.9 (0.0, 11.7)	16.3 (8.8, 25.1)	<0.001
Core mass, g	1.2 (0.0, 3.4)	0.9 (0.0, 2.9)	5.2 (2.9, 9.0)	<0.001
Core/LV mass ratio (%)	0.9 (0.0, 2.1)	0.8 (0.0, 1.9)	2.5 (1.8, 3.7)	<0.001
BZ channels + patients, *n* (%)	140 (34.1%)	117 (30.5%)	23 (88.5%)	<0.001
BZ channel mass, g	0.0 (0.0, 0.7)	0.0 (0.0, 0.5)	2.1 (1.2, 3.4)	<0.001
BZ channel mass/LV mass (%)	0.0 (0.0, 0.5)	0.0 (0.0, 0.4)	1.0 (0.6, 2.0)	<0.001

BZ, borderzone; LGE, late gadolinium enhancement; LV, left ventricular

of LGE + patients, respectively), followed by basal anterior and anteroseptal (segments 1 and 2; 29% and 33% of LGE + patients, respectively). In the whole population, median scar mass was 9.7 g (IQR 0.0–22.3), representing 7.3% (IQR 0.0–14.3) of LV mass. The scar was composed of a median of 8.0 g (IQR 0.0–19.2) of BZ tissue and of 1.2 g (IQR 0.0–3.4) of dense core (*Table 2*). These two components constituted 6.4% (IQR 0.0–12.2) and 0.9% (IQR 0.0–2.1) of LV mass, respectively.

BZ channels were found in 140 patients (34.1% of the whole population, 47.0% of LGE + patients). Most patients ($n = 72$; 51.4%) had only 1 BZ channel, 32 (22.9%) patients had 2 BZ channels, and 36 (25.7%) patients had >2 BZ channels. Out of 294 identified BZ channels, the majority were mid-myocardial ($n = 102$; 34.7%) or epicardial ($n = 98$, 33.3%), while 59 (20.1%) were endocardial-only, and a minority ($n = 35$; 11.9%) were transmural. Among patients with BZ channels, the median channel mass was 1.54 g (IQR 0.71–3.36), representing 0.88% (IQR 0.50–1.83) of LV mass. The correlation between scar mass and BZ channels mass was significant but moderate, with a Pearson's correlation coefficient (r) of 0.64 ($R^2 = 0.41$; $P < 0.001$), indicating substantial yet variable structural relationship between dense scar and BZ components in the formation of BZ channels. (*Figure 2*).

Clinical profiles and scar composition

Patients with massive LV hypertrophy (13.8%, IQR 8.3–21.2% vs. 6.5%, IQR 0.0–13.2; $P < 0.001$) and those with LV systolic dysfunction (17.9%, IQR 10.9–28.2% vs. 7.0%, IQR 0.0–13.7; $P < 0.001$) had the highest scar

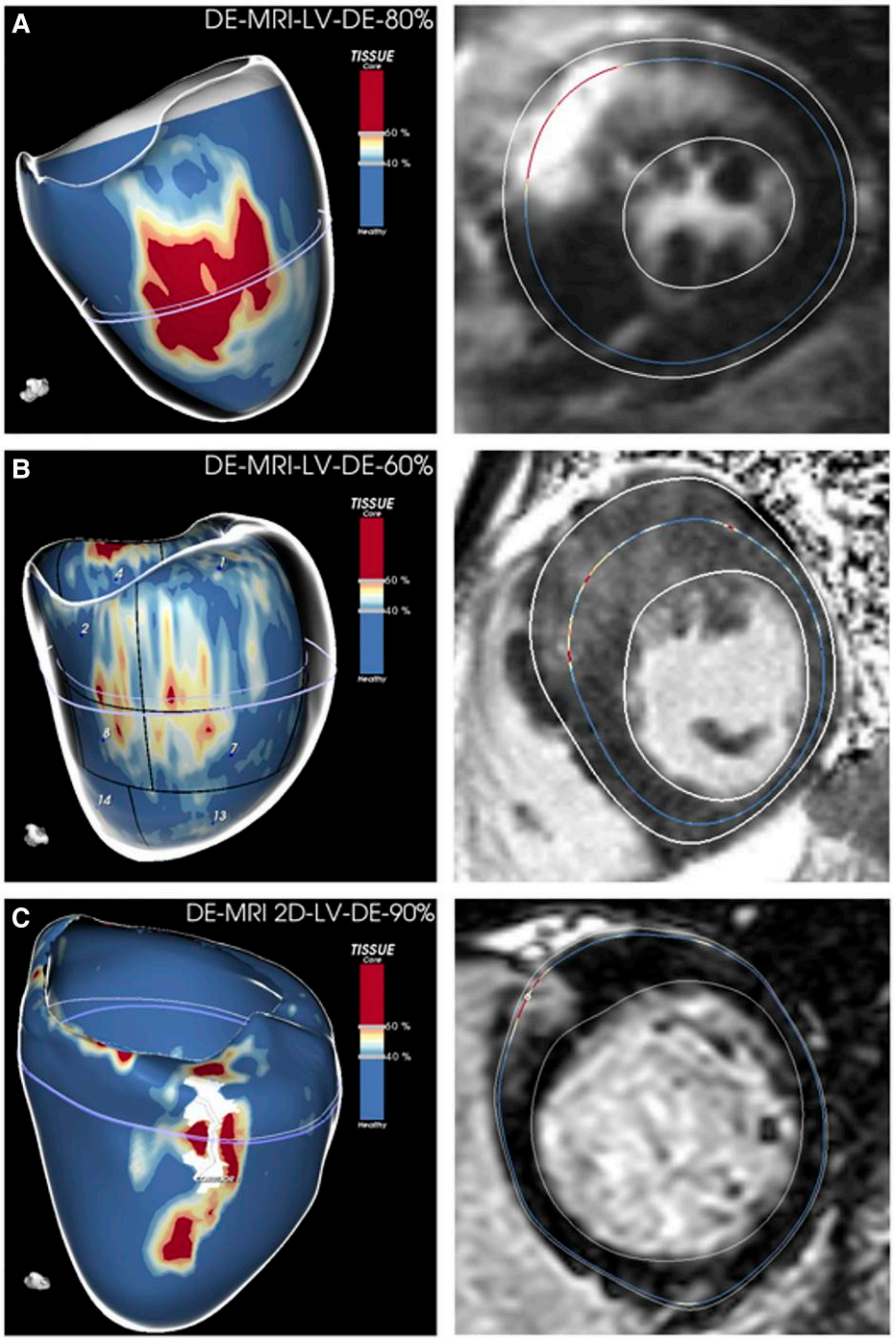

Figure 2 Scar and BZ channels mass. Patients with extensive homogeneous dense scar may lack sufficient BZ tissue to create channels (*A*), while those with diffuse BZ fibrosis may have insufficient dense scar to protect the channel (*B*). Small but heterogeneous scars may contain strands of BZ tissue that are sufficiently protected to form BZ channels (*C*).

burden and prevalence of BZ channels (50.0% vs. 32.1%; $P = 0.01$ and 73.1% vs. 31.5%; $P < 0.001$, respectively). (*Figure 3*, panels A and B). The prevalence of massive hypertrophy, NSVT, LV systolic dysfunction, and atrial fibrillation was significantly higher in patients with BZ channels (*Table 3*).

Primary endpoint

During a median follow-up of 65 months (IQR: 36–95) after CMR, 26 (6.3%) patients reached the VT/VF endpoint (5-year cumulative rate: 4.9%; 95% CI: 2.6–7.9). Among 137 patients who had an ICD implanted, 20 had appropriate interventions (12 polymorphic VT/VF and 8 monomorphic VTs). Among non-ICD carriers ($n = 276$) 5 patients died suddenly, and 1 had resuscitated cardiac arrest. Total scar, BZ and core mass were all significantly higher in VT/VF patients (*Table 2* and *Figure 4*). BZ channels were observed in 88.5% of patients with VT/VF compared with 30.5% of those without ($P < 0.001$), with the BZ channels mass being significantly higher in the VT/VF group (*Table 2*).

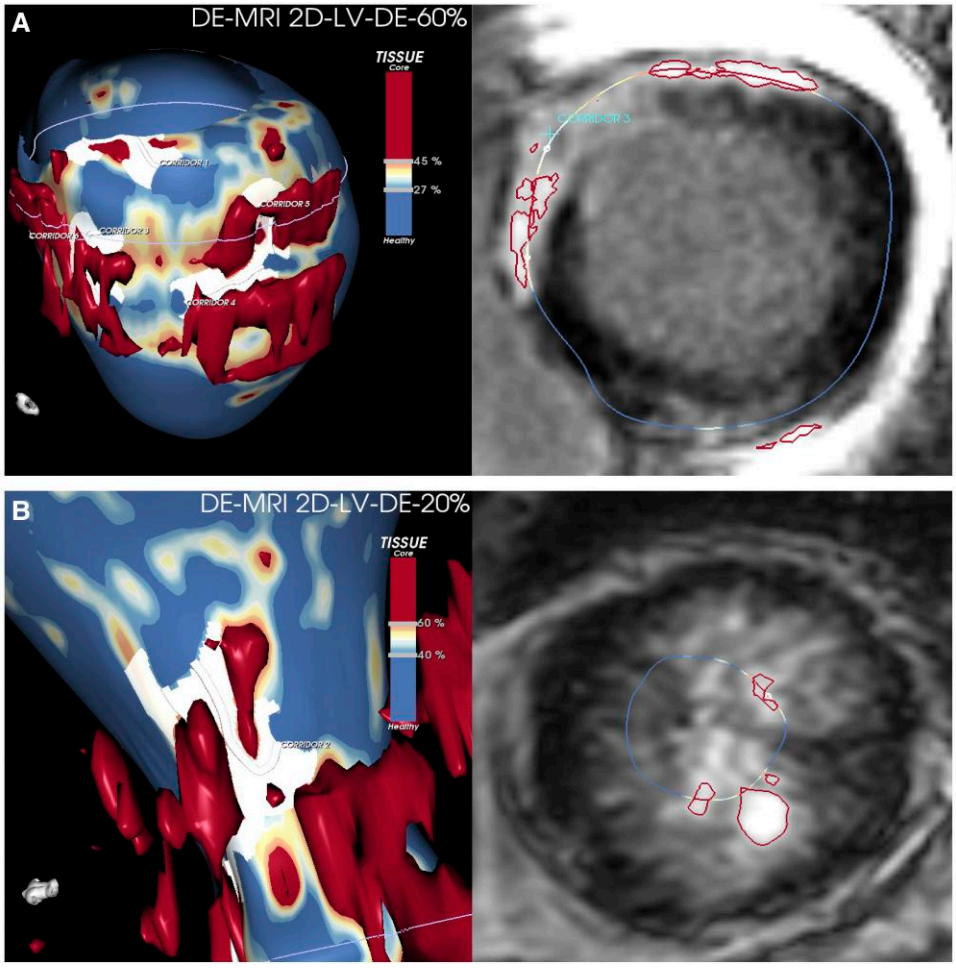

Figure 3 Scar patterns and clinical profiles. CMR short-axis view and three-dimensional reconstruction of scar architecture in an HCM patient with LV systolic dysfunction (*A*) and of another with massive hypertrophy involving the LV apex (*B*). Both phenotypes showed higher scar mass and prevalence of BZ channels.

Table 3 Comparison of clinical characteristics of HCM patients with and without BZ channels

Characteristics	All ($n = 410$)	BZ channels − ($n = 270$)	BZ channels + ($n = 140$)	*P*
Male sex, *n* (%)	273 (66.6%)	178 (65.9%)	95 (67.9%)	0.741
Age at CMR (years)	55.0 (41.0, 64.8)	54.0 (39.2, 64.0)	56.0 (44.8, 65.0)	0.177
Clinical				
LVOT gradient ≥30 mm Hg	81 (19.8%)	56 (20.7%)	25 (17.9%)	0.516
Atrial fibrillation, *n* (%)	64 (15.6%)	28 (10.4%)	36 (25.7%)	<0.001
Risk factors				
Unexplained syncope, *n* (%)	33 (8.0%)	22 (8.1%)	11 (7.9%)	0.992
Family history of SD, *n* (%)	65 (15.9%)	38 (14.1%)	27 (19.3%)	0.199
Max wall thickness (mm)	18.0 (16.0, 22.0)	18.0 (16.0, 22.0)	20.0 (17.0, 24.0)	<0.001
Max wall thickness >30 mm, *n* (%)	44 (10.7%)	21 (7.8%)	23 (16.4%)	0.011
NSVT, *n* (%)	123 (30.0%)	70 (25.9%)	53 (37.9%)	0.017
Apical aneurysm, *n* (%)	15 (3.7%)	10 (3.7%)	5 (3.6%)	0.997
EF <50%, *n* (%)	26 (6.3%)	7 (2.6%)	19 (13.6%)	<0.001
ESC 5-years risk of SD (%)	2.4 (1.6, 4.4)	2.2 (1.5, 4.0)	3.1 (1.7, 4.8)	0.002

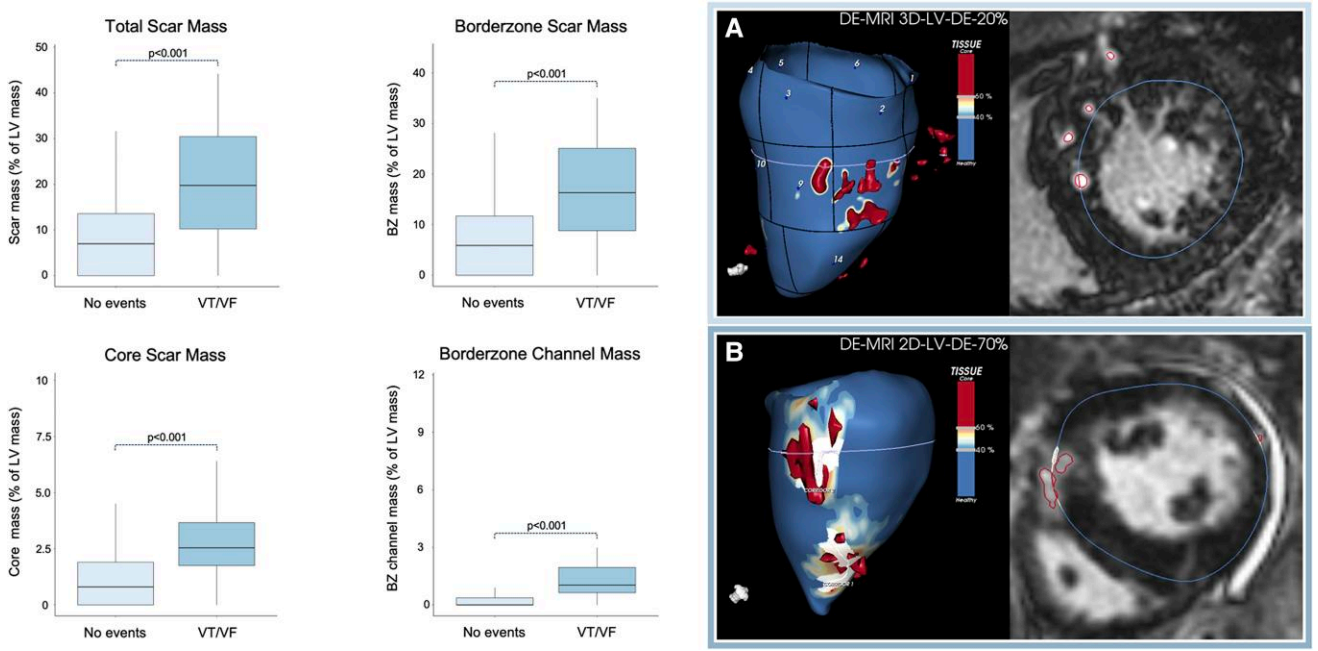

Figure 4 Scar architecture in patients with vs. without VA. Left box plots comparing scar mass, BZ mass, core mass and BZ channel mass in patients with vs. without VT/VF. Right (*A*) CMR of a patient with low burden and spotty LGE who did not experience VA. (*B*) CMR of a patient with septal LV scar and multiple BZ channels who experienced VT.

The 5-year cumulative rate of VT/VF events was significantly higher among patients with (14.0%, 95% CI: 7.2–20.3) vs. without (0.6%; 95% CI: 0.1–1.7) BZ channels ($P < 0.0001$) (*Figure 5*, panel A). BZ channel mass was independently associated with a high risk of VT/VF after adjustment for both ESC (HR: 1.45; 95% CI: 1.26–1.67; $P < 0.0001$) and AHA/ACC (HR: 1.34; 95% CI: 1.16–1.54; $P < 0.0001$) risk estimate.

Prediction models

Based on the area under the ROC curve (AUC), scar mass, BZ mass, core mass, and BZ channel mass correctly classified the primary endpoint of VT/VF, with BZ channel mass emerging as the best discriminator (AUC: 0.82; 95% CI 0.74–0.89; $P < 0.001$) (*Figure 5*, panel B). Out of 10 LGE + patients who experienced VT/VF despite scar mass <15%, 9 had BZ channels. Indeed, among patients with scar burden <15%, the 5 year-cumulative event rate was 9.7% (95% CI: 1.0–17.7) in patients with BZ channels vs. 0.6% (95% CI: 0.01–1.9) in those without ($P < 0.001$).

The AUC value for BZ channels (binary variable) was higher (0.79; 95% CI: 0.72–0.85; $P < 0.001$) as compared to the ESC (0.71; 95% CI: 0.61–0.81; $P < 0.001$) or AHA/ACC (0.72; 95% CI: 0.64–0.81; $P < 0.001$) models. Integrating BZ channels with the ESC or the ACC/AHA models significantly improved their AUC to 0.86 (95% CI: 0.80–0.92; $P < 0.001$), and to 0.85 (95% CI: 0.79–0.92; $P < 0.001$), respectively.

Reclassification analysis

According to the ESC guidelines, 72 (17.6%) patients were high risk (Class I/IIa indication), while 338 (82.4%) patients were low-risk (Class IIb or no indication). Adding BZ channel mass to the ESC model improved risk stratification (NRI: 0.19; 95% CI: 0.01–0.37; $P = 0.03$), reclassifying upward 8 VT/VF patients (+30%) and 44 patients without events (+11%), with no incorrect downward reclassifications. Among 338 low-risk patients, 11 had VT/VF, 10 of who had BZ channels. According to AHA/ACC guidelines, 142 (34.6%) patients were high risk and 268 (65.4%) low risk. Adding BZ channel mass to the AHA/ACC model improved risk stratification (NRI: 0.32; 95% CI: 0.13–0.51; $P < 0.001$), reclassifying upward 10 VT/VF patients (+38%) and 23 patients without events (+6%), with no incorrect downward reclassifications. Among 268 low-risk patients, 6 had VT/VF, 5 of who had BZ channels.

Discussion

The prevention of SCD with ICDs has revolutionized HCM management.[20] Conventional risk factors and prediction models have proven highly effective in identifying high risk patients. Despite advances minimizing ICD-related risks,[21,22] refining risk stratification remains essential. Among novel risk factors,[8] the magnitude of scar mass is as a strong predictor of SCD. Notwithstanding this, complex extracellular matrix remodeling, as evidenced by LGE texture heterogeneity, is associated with higher risk of VA[9,10] and may reflect a distinct arrhythmic substrate. Indeed, three-dimensional scar architecture has been shown to predict ICD interventions in high-risk HCM patients[14] and affect the electrophysiological characteristics of induced VA.[23] In the present study, we assessed a cohort of unselected HCM patients to describe scar architecture, report on possible correlations between scar structural patterns and clinical profiles, and define whether scar composition might be relevant to the risk of VA. The main findings are that (i) HCM patients display peculiar LGE composition, showing predominance of BZ tissue and relatively common protected BZ channels within the scar, serving as possible substrates for reentrant arrhythmia; (ii) HCM patients with LV systolic dysfunction and massive hypertrophy present a distinct scar architecture, with higher mass of BZ channels; (iii) BZ channels predict the risk of VT/VF independently from classic risk factors; (iv) assessment of BZ channels improves the performance of the ESC and AHA models that rely on traditional risk factors.

Scar architecture in HCM

Myocardial fibrosis is a hallmark of HCM and a common finding in necropsies of young SCD victims.[24] LGE, representing replacement fibrosis histologically, is present in 33–84% of HCM patients either in focal or diffuse patchy mid-myocardial distribution, depending on clinical phenotypes and disease severity.[25]

In ischemic cardiomyopathy, dense scar with embedded viable myocardial fibers supports re-entrant VA.[26,27] Of note, HCM is pathologically different, showing more diffuse fibrosis combined with viable muscle fibers rather than dense scarring in a particular vascular territory.[28–30] Compared with post-myocardial infarction patients,[13,27,31] our HCM cohort displayed scars richer in BZ tissue and less dense scar, aligning with prior reports that most LGE in HCM reflects subtle rather than replacement fibrosis.[30] Moreover, while scarring is mainly subendocardial in ischemic heart disease, LGE was predominantly mid-myocardial in our as well as in other HCM cohorts.[32] Of note, we identified BZ channels in only one third of patients, with lower mass than in myocardial infarction[13] or severe LV dysfunction.[12] However, high-risk phenotypes (massive hypertrophy, LV dysfunction) had greater BZ channel mass, closely related to overall BZ and core scar extent.

Scar composition and ventricular arrhythmia

Scars are substrates for reentrant arrhythmias, and LGE is an established risk factor for VA and SCD in HCM.[3,33,34] Indeed, bipolar electrograms from LGE areas show low amplitude and prolonged signals, indicating conduction delay[35] and slowly conducting viable myocardium within scarred areas (BZ channels), providing the milieu for rapid-rate reentrant VTs. These arrhythmias may then convert into polymorphic VT or VF due to the specific features of the HCM myocardium, which is characterized by sarcomeric misalignment and non-uniform anisotropic conduction.[36]

BZ channels have been associated with higher VA risk in MI, severe LV dysfunction,[12,13,27] and high-risk HCM.[14] Our findings extend this concept to all LGE positive HCM patients and may offer a mechanistic explanation for the increased risk of VA that is associated with scar heterogeneity.[5,10] Unlike other approaches to quantify non-homogeneous scar patterns (e.g. LGE-dispersion mapping, entropy, or radiomics,[5,9,10] which provide prognostic value without addressing scar architecture, 3D reconstruction of core, BZ, and BZ channels directly relates tissue heterogeneity to a pathophysiological model).

In agreement with previous observations,[3,4,32,37,38] scar burden predicted VT/VF in our study. In large analyses, SCD risk peaked with scar mass ≥15%, while minimal LGE (1–5%) was not significantly different from no LGE.[3] In our cohort, BZ channels distinguished patients with and without VT/VF, and their mass was a strong predictor of events. Scar mass and BZ channel mass were moderately correlated, indicating partial dependence but also independent variability. Indeed, large scars do not always have high BZ density, while even small scars can be highly arrhythmogenic if they have the proper BZ–dense scar architecture. In line with this, a more conservative LGE 10% cutoff could re-stratify intermediate-risk patients.[39] Notably, 9/10 LGE-positive patients with VT/VF and scar <15% had protected BZ channels, further supporting this concept. The inclusion of BZ channels as an additional parameter improved both the ESC and AHA/ACC risk models, with higher AUC and NRI, providing prognostic information beyond that currently available. Although patients were enrolled at tertiary centres, the 5-year cumulative VT/VF rate and the overall clinical profile align with unselected HCM cohorts. Notably, the association between BZ channels

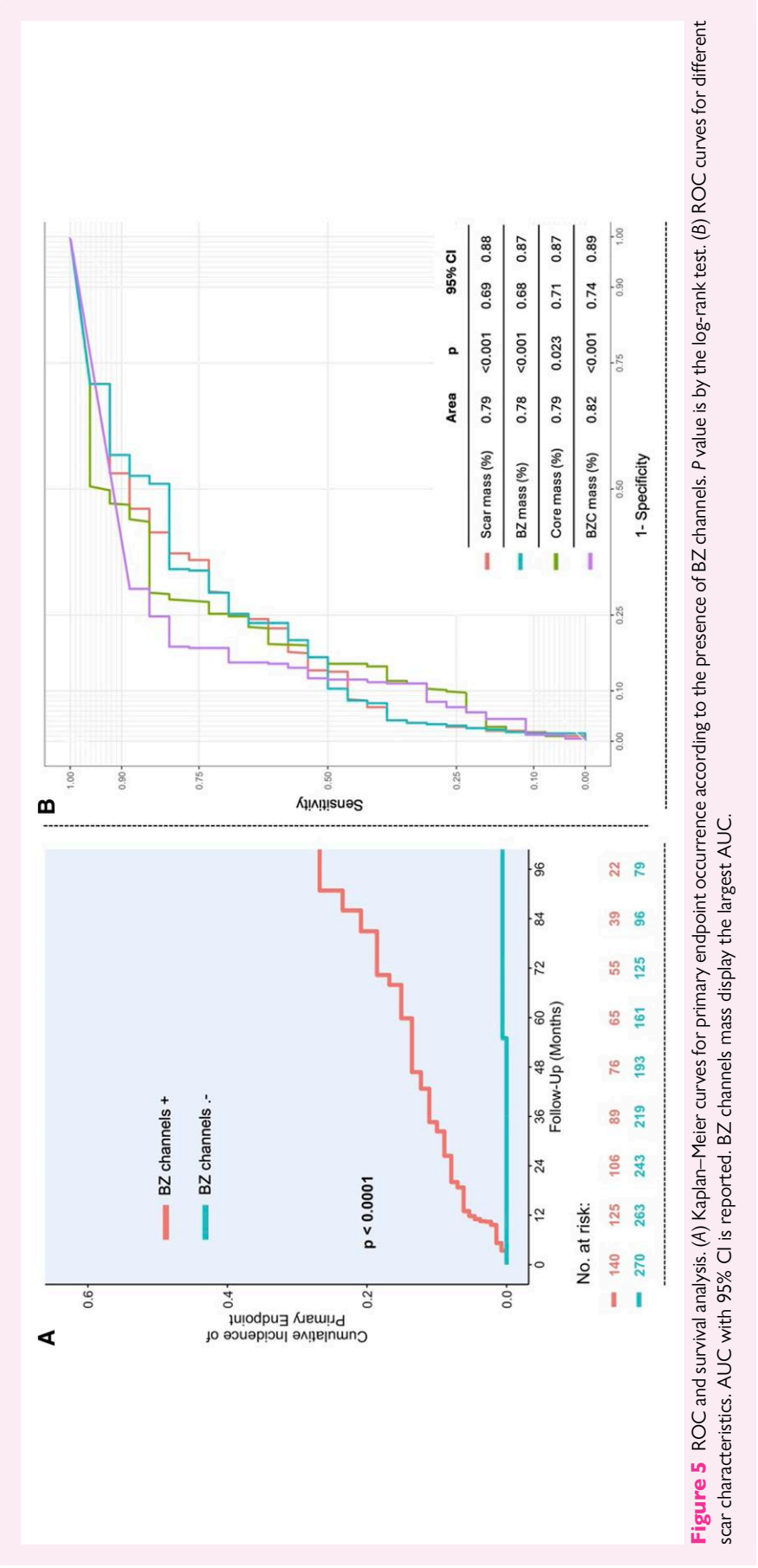

Figure 5 ROC and survival analysis. (*A*) Kaplan–Meier curves for primary endpoint occurrence according to the presence of BZ channels. *P* value is by the log-rank test. (*B*) ROC curves for different scar characteristics. AUC with 95% CI is reported. BZ channels mass display the largest AUC.

and VT/VF persisted after adjustment for guideline-defined high-risk status and was evident within ESC low-risk strata, supporting the potential applicability of substrate-based risk markers beyond the high-risk setting. Nevertheless, extrapolation to community cohorts requires prospective, population-based validation and, ideally, serial-CMR studies to capture dynamic scar remodelling.

Of note, we highlight scar-related reentry as the primary arrhythmogenic mechanism underlying VA in HCM. Nonetheless, it is well recognized that VA can occur in HCM patients who exhibit either no or minimal LGE. In these patients, pathological changes in ion currents and intracellular Ca^{2+} homeostasis may represent the primary arrhythmogenic mechanism.[40] Although our study does not account for the contribution of molecular and cellular mechanisms, it provides a conceptual framework for VA pathophysiology in HCM. It should also be acknowledged that HCM-related scars remodel over time.[41,42] This dynamic process, which was not fully accounted for in the present analysis, may influence long-term arrhythmic risk and limit the accuracy of risk stratification when based on a single time-point assessment. In this context, serial CMRs could provide a more dynamic approach to risk stratification and may capture the evolving scar architecture and composition over time.

Study limitations

This study has several limitations. First, its retrospective design may be affected by selection bias and unrecognized confounders. Second, although one previous study demonstrated that scar composition has predictive value in a high-risk HCM cohort,[14] establishing its role in a community-based population with a low prevalence of LGE, few ICD carriers, and a low event rate remains challenging; nonetheless, despite being entirely derived from tertiary centres, our cohort displayed clinical features and overall risk consistent with an unselected HCM population. Third, CMR scans were performed on different scanners and with variable protocols, which may affect scar characterization and BZ channel assessment. Although scar composition is sensitive to PSI thresholds and reconstruction type,[43] channel mass remains relatively stable.[44] In this study, all analyses were performed on magnitude reconstructions, minimizing systematic bias, and the predominance of 1.5 T 2D acquisitions supports generalizability. However, clinical implementation of scar assessment for risk stratification will require harmonization of key methodological aspects, such as field strength, reconstruction type, segmentation thresholds, and standardized reporting of scar metrics. Different post-processing platforms are clinically viable, with optimal use depending on available imaging, institutional resources, and the balance between automation and operator input.[45] Fourth, the ADAS-3D FWHM-based algorithm was originally validated in ischaemic substrates, and formal disease-specific validation in HCM is lacking. Although supporting evidence exists in non-ischaemic conditions[12] and we previously reported concordance between channel architecture, VT inducibility, and ECG features in HCM,[23] these findings do not substitute for HCM-specific validation. Therefore, interpretation should consider this limitation. Fifth, the limited number of primary events and predominance of ICD therapies reduce statistical power and may affect model stability. This limitation is acknowledged, and the findings should be interpreted with caution. Finally, genetic testing was not addressed. Prior studies indicate that sarcomere gene mutations influence LGE burden and remodeling.[46] It is likely that specific mutations may affect the electrophysiological properties of border zone tissue, thereby modulating arrhythmic substrate, which represents an important area for future research.

Conclusions

This study provides a mechanistic explanation for the higher VA risk associated with scar heterogeneity in HCM, showing that spatial organization of BZ tissue in protected channels strongly predicts VA and adds prognostic value beyond current models. Myocardial scar architecture may serve as a structural biomarker for VA risk, supporting a more nuanced approach to LGE evaluation in HCM. While conventional models effectively identify high-risk patients and guide ICD therapy, integrating substrate assessment could enhance their performance and contribute to a more personalized definition of the arrhythmic risk.

Author contributions

Pietro Francia (Conceptualization [lead]; Data curation [lead]; Formal analysis [lead]; Investigation [lead]; Methodology [lead]; Project administration [lead]; Software [lead]; Writing—original draft [lead]; Writing—review & editing [lead]), Julio Martì-Almor (Methodology [lead]; Supervision [lead]; Writing—review & editing [lead]), Andrea Saglietto (Data curation [equal]; Formal analysis [lead]; Investigation [equal]; Methodology [equal]; Software [equal]; Writing—review & editing [equal]), Raffaello Ditaranto (Data curation [equal]; Investigation [lead]; Methodology [lead]), Paula Franco-Ocaña (Formal analysis [equal]; Investigation [lead]; Methodology [equal]; Software [lead]), David Soto-Iglesias (Data curation [lead]; Formal analysis [equal]; Investigation [equal]; Methodology [lead]; Software [lead]), Cristina Panico (Formal analysis [equal]; Investigation [lead]; Methodology [lead]), Guido del Monaco (Data curation [equal]; Formal analysis [lead]; Investigation [equal]; Methodology [equal]), Sebastiano Carli (Data curation [equal]; Formal analysis [equal]; Investigation [lead]; Methodology [equal]), Camillo Autore (Conceptualization [equal]; Methodology [equal]; Supervision [lead]; Writing—original draft [lead]; Writing—review & editing [lead]), Rita Amador (Data curation [equal]; Investigation [lead]; Methodology [lead]), Matteo Sclafani (Data curation [lead]; Investigation [lead]; Methodology [equal]; Writing—review & editing [equal]), Giacomo Tini (Data curation [lead]; Investigation [lead]; Methodology [lead]; Writing—original draft [equal]), José Tomás Ortiz-Pérez (Data curation [lead]; Formal analysis [lead]; Investigation [lead]; Methodology [lead]; Writing—review & editing [lead]), Diego Penela (Conceptualization [equal]; Data curation [lead]; Investigation [lead]; Methodology [lead]; Supervision [lead]; Writing—review & editing [lead]), Pedro Freitas (Data curation [lead]; Investigation [lead]; Methodology [lead]; Supervision [lead]; Validation [lead]; Writing—review & editing [lead]), Elena Biagini (Conceptualization [lead]; Data curation [lead]; Supervision [lead]; Writing—review & editing [lead]), Maria Beatrice Musumeci (Conceptualization [equal]; Data curation [lead]; Investigation [lead]; Methodology [lead]; Writing—review & editing [equal]), Giulio Falasconi (Data curation [lead]; Formal analysis [lead]; Methodology [equal]; Validation [equal]; Writing—original draft [equal]), Maria Alessandra Schiavo (Data curation [lead]; Investigation [equal]; Methodology [equal]), and Antonio Berruezo (Conceptualization [lead]; Investigation [lead]; Methodology [lead]; Project administration [lead]; Supervision [lead]; Writing—original draft [lead]; Writing—review & editing [lead])

Funding

This work was supported in part by the Italian Ministry of Health (RC-2024-2789983) and from University Sapienza (RM12117A8ABD4220).

Conflict of interest: P.F. received speaker fees from Boston Scientific and research grants from Abbott and Boston Scientific. A.B. is stockholder of Galgo Medical. D.S.-I. and P.F.-O. are employees of Biosense Webster Inc. All other authors declared no conflicts of interest.

Data availability

The data that support the findings of this study are available from the corresponding author upon reasonable request.

References

1. Greulich S, Schumm J, Grün S, Bruder O, Sechtem U, Mahrholdt H. Incremental value of late gadolinium enhancement for management of patients with hypertrophic cardiomyopathy. *Am J Cardiol* 2012;**110**:1207–12.
2. Ho CY, López B, Coelho-Filho OR, Lakdawala NK, Cirino AL, Jarolim P *et al.* Myocardial fibrosis as an early manifestation of hypertrophic cardiomyopathy. *N Engl J Med* 2010; **363**:552–63.
3. Chan RH, Maron BJ, Olivotto I, Pencina MJ, Assenza GE, Haas T *et al.* Prognostic value of quantitative contrast-enhanced cardiovascular magnetic resonance for the evaluation of sudden death risk in patients with hypertrophic cardiomyopathy. *Circulation* 2014;**130**: 484–95.
4. Kwon DH, Smedira NG, Rodriguez ER, Tan C, Setser R, Thamilarasan M *et al.* Cardiac magnetic resonance detection of myocardial scarring in hypertrophic cardiomyopathy: correlation with histopathology and prevalence of ventricular tachycardia. *J Am Coll Cardiol* 2009;**54**:242–9.
5. Ye Y, Ji Z, Zhou W, Pu C, Li Y, Zhou C *et al.* Mean scar entropy by late gadolinium enhancement cardiac magnetic resonance is associated with ventricular arrhythmias events in hypertrophic cardiomyopathy. *Front Cardiovasc Med* 2021;**8**:758635.
6. Appelbaum E, Maron BJ, Adabag S, Hauser TH, Lesser JR, Haas TS *et al.* Intermediate-signal-intensity late gadolinium enhancement predicts ventricular tachyarrhythmias in patients with hypertrophic cardiomyopathy. *Circ Cardiovasc Imaging* 2012; **5**:78–85.
7. Zeppenfeld K, Tfelt-Hansen J, de Riva M, Winkel BG, Behr ER, Blom NA *et al.* 2022 ESC guidelines for the management of patients with ventricular arrhythmias and the prevention of sudden cardiac death. *Eur Heart J* 2022;**43**:3997–4126.
8. Ommen SR, Ho CY, Asif IM, Balaji S, Burke MA, Day SM *et al.* 2024 AHA/ACC/AMSSM/HRS/PACES/SCMR guideline for the management of hypertrophic cardiomyopathy: a report of the American Heart Association/American College of Cardiology joint committee on clinical practice guidelines. *J Am Coll Cardiol* 2024;**83**:2324–405.
9. Aquaro GD, Grigoratos C, Bracco A, Proclemer A, Todiere G, Martini N *et al.* Late gadolinium enhancement-dispersion mapping: a new magnetic resonance imaging technique to assess prognosis in patients with hypertrophic cardiomyopathy and low-intermediate 5-year risk of sudden death. *Circ Cardiovasc Imaging* 2020;**13**:e010489.
10. Fahmy AS, Rowin EJ, Jaafar N, Chan RH, Rodriguez J, Nakamori S *et al.* Radiomics of late gadolinium enhancement reveals prognostic value of myocardial scar heterogeneity in hypertrophic cardiomyopathy. *JACC Cardiovasc Imaging* 2023;**17**:16–27.
11. Heidary S, Patel H, Chung J, Yokota H, Gupta SN, Bennett MV *et al.* Quantitative tissue characterization of infarct core and border zone in patients with ischemic cardiomyopathy by magnetic resonance is associated with future cardiovascular events. *J Am Coll Cardiol* 2010;**55**:2762–8.
12. Acosta J, Fernández-Armenta J, Borràs R, Anguera I, Bisbal F, Martí-Almor J *et al.* Scar characterization to predict life-threatening arrhythmic events and sudden cardiac death in patients with cardiac resynchronization therapy: the GAUDI-CRT study. *JACC Cardiovasc Imaging* 2018;**11**:561–72.
13. Jáuregui B, Soto-Iglesias D, Penela D, Acosta J, Fernández-Armenta J, Linhart M *et al.* Cardiovascular magnetic resonance determinants of ventricular arrhythmic events after myocardial infarction. *Europace* 2021;**24**:938–47.
14. Francia P, Ocaña-Franco P, Cristiano E, Falasconi G, Adduci C, Soto-Iglesias D *et al.* Substrates of scar-related ventricular arrhythmia in patients with hypertrophic cardiomyopathy: a cardiac magnetic resonance study. *JACC Cardiovasc Imaging* 2023;**16**: 1359–62.
15. Elliott PM, Anastasakis A, Borger MA, Borggrefe M, Cecchi F, Charron P *et al.* 2014 ESC guidelines on diagnosis and management of hypertrophic cardiomyopathy: the task force for the diagnosis and management of hypertrophic cardiomyopathy of the European Society of Cardiology (ESC). *Eur Heart J* 2014;**35**:2733–79.
16. Ommen SR, Ho CY, Asif IM, Balaji S, Burke MA, Day SM *et al.* 2024 AHA/ACC/AMSSM/HRS/PACES/SCMR guideline for the management of hypertrophic cardiomyopathy: a report of the American Heart Association/American College of Cardiology joint committee on clinical practice Guidelines. *Circulation* 2024;**149**:e1239–311.
17. Andreu D, Ortiz-Pérez JT, Fernández-Armenta J, Guiu E, Acosta J, Prat-González S *et al.* 3D delayed-enhanced magnetic resonance sequences improve conducting channel delineation prior to ventricular tachycardia ablation. *Europace* 2015;**17**:938–45.
18. Fernández-Armenta J, Berruezo A, Andreu D, Camara O, Silva E, Serra L *et al.* Three-dimensional architecture of scar and conducting channels based on high resolution ce-CMR: insights for ventricular tachycardia ablation. *Circ Arrhythm Electrophysiol* 2013;**6**:528–37.
19. Norrish G, Ding T, Field E, McLeod K, Ilina M, Stuart G *et al.* A validation study of the European Society of Cardiology guidelines for risk stratification of sudden cardiac death in childhood hypertrophic cardiomyopathy. *Europace* 2019;**21**:1559–65.
20. Maron BJ, Casey SA, Olivotto I, Sherrid MV, Semsarian C, Autore C *et al.* Clinical course and quality of life in high-risk patients with hypertrophic cardiomyopathy and implantable cardioverter-defibrillators. *Circ Arrhythm Electrophysiol* 2018;**11**: e005820.
21. Francia P, Ziacchi M, Adduci C, Ammendola E, Pieragnoli P, De Filippo P *et al.* Clinical course of hypertrophic cardiomyopathy patients implanted with a transvenous or subcutaneous defibrillator. *Europace* 2023;**25**:euad270.
22. Francia P, Olivotto I, Lambiase PD, Autore C. Implantable cardioverter-defibrillators for hypertrophic cardiomyopathy: the times they are a-changin'. *Europace* 2021;**24**: 1384–94.
23. Francia P, Falasconi G, Penela D, Viveros D, Alderete J, Saglietto A *et al.* Scar architecture affects the electrophysiological characteristics of induced ventricular arrhythmias in hypertrophic cardiomyopathy. *Europace* 2024;**26**:euae050.
24. Basso C, Thiene G, Corrado D, Buja G, Melacini P, Nava A. Hypertrophic cardiomyopathy and sudden death in the young: pathologic evidence of myocardial ischemia. *Hum Pathol* 2000;**31**:988–98.
25. Moon JC, McKenna WJ, McCrohon JA, Elliott PM, Smith GC, Pennell DJ. Toward clinical risk assessment in hypertrophic cardiomyopathy with gadolinium cardiovascular magnetic resonance. *J Am Coll Cardiol* 2003;**41**:1561–7.
26. de Bakker JM, van Capelle FJ, Janse MJ, Wilde AA, Coronel R, Becker AE *et al.* Reentry as a cause of ventricular tachycardia in patients with chronic ischemic heart disease: electrophysiologic and anatomic correlation. *Circulation* 1988;**77**:589–606.
27. Bhagirath P, Campos FO, Zaidi HA, Chen Z, Elliott M, Gould J *et al.* Predicting postinfarct ventricular tachycardia by integrating cardiac MRI and advanced computational reentrant pathway analysis. *Heart Rhythm* 2024;**21**:1962–9.
28. Foà A, Agostini V, Rapezzi C, Olivotto I, Corti B, Potena L *et al.* Histopathological comparison of intramural coronary artery remodeling and myocardial fibrosis in obstructive versus end-stage hypertrophic cardiomyopathy. *Int J Cardiol* 2019;**291**: 77–82.
29. Konno T, Hayashi K, Fujino N, Nagata Y, Hodatsu A, Masuta E *et al.* High sensitivity of late gadolinium enhancement for predicting microscopic myocardial scarring in biopsied specimens in hypertrophic cardiomyopathy. *PLoS One* 2014;**9**:e101465.
30. Moravsky G, Ofek E, Rakowski H, Butany J, Williams L, Ralph-Edwards A *et al.* Myocardial fibrosis in hypertrophic cardiomyopathy: accurate reflection of histopathological findings by CMR. *JACC Cardiovasc Imaging* 2013;**6**:587–96.
31. Jones RE, Zaidi HA, Hammersley DJ, Hatipoglu S, Owen R, Balaban G *et al.* Comprehensive phenotypic characterization of late gadolinium enhancement predicts sudden cardiac death in coronary artery disease. *JACC Cardiovasc Imaging* 2023;**16**: 628–38.
32. Bruder O, Wagner A, Jensen CJ, Schneider S, Ong P, Kispert EM *et al.* Myocardial scar visualized by cardiovascular magnetic resonance imaging predicts major adverse events in patients with hypertrophic cardiomyopathy. *J Am Coll Cardiol* 2010;**56**:875–87.
33. Rowin EJ, Maron MS, Adler A, Albano AJ, Varnava AM, Spears D *et al.* Importance of newer cardiac magnetic resonance-based risk markers for sudden death prevention in hypertrophic cardiomyopathy:an international multicenter study. *Heart Rhythm* 2021;**19**:782–9.
34. Sclafani M, Falasconi G, Tini G, Musumeci B, Penela D, Saglietto A *et al.* Substrates of sudden cardiac death in hypertrophic cardiomyopathy. *J Clin Med* 2025;**14**: 1331.
35. Sakamoto N, Kawamura Y, Sato N, Nimura A, Matsuki M, Yamauchi A *et al.* Late gadolinium enhancement on cardiac magnetic resonance represents the depolarizing and repolarizing electrically damaged foci causing malignant ventricular arrhythmia in hypertrophic cardiomyopathy. *Heart Rhythm* 2015;**12**:1276–84.
36. Perez-Alday EA, Haq KT, German DM, Hamilton C, Johnson K, Phan F *et al.* Mechanisms of arrhythmogenicity in hypertrophic cardiomyopathy: insight from non-invasive electrocardiographic imaging. *Front Physiol* 2020;**11**:344.
37. Rubinshtein R, Glockner JF, Ommen SR, Araoz PA, Ackerman MJ, Sorajja P *et al.* Characteristics and clinical significance of late gadolinium enhancement by contrast-enhanced magnetic resonance imaging in patients with hypertrophic cardiomyopathy. *Circ Heart Fail* 2010;**3**:51–8.
38. Suk T, Edwards C, Hart H, Christiansen JP. Myocardial scar detected by contrast-enhanced cardiac magnetic resonance imaging is associated with ventricular tachycardia in hypertrophic cardiomyopathy patients. *Heart Lung Circ* 2008;**17**:370–4.
39. Kiaos A, Daskalopoulos GN, Kamperidis V, Ziakas A, Efthimiadis G, Karamitsos TD. Quantitative late gadolinium enhancement cardiac magnetic resonance and sudden death in hypertrophic cardiomyopathy: a meta-analysis. *JACC Cardiovasc Imaging* 2024; **17**:489–97.
40. Coppini R, Santini L, Olivotto I, Ackerman MJ, Cerbai E. Abnormalities in sodium current and calcium homoeostasis as drivers of arrhythmogenesis in hypertrophic cardiomyopathy. *Cardiovasc Res* 2020;**116**:1585–99.
41. Habib M, Adler A, Fardfini K, Hoss S, Hanneman K, Rowin EJ *et al.* Progression of myocardial fibrosis in hypertrophic cardiomyopathy: a cardiac magnetic resonance study. *JACC Cardiovasc Imaging* 2021;**14**:947–58.

42. Aquaro GD, Todiere G, Barison A, Grigoratos C, Parisella ML, Adami M *et al.* Prognostic role of the progression of late gadolinium enhancement in hypertrophic cardiomyopathy. *Am J Cardiol* 2024;**211**:199–208.
43. Burger JC, Hopman L, Campos FO, Allaart CP, Postema PG, Kemme MJB *et al.* Optimizing ventricular scar characterization in late-gadolinium enhancement cardiac MRI: impact of thresholding techniques in magnitude and phase-sensitive reconstructed images. *Heart Rhythm* 2025;**22**:2469–76.
44. Bhagirath P, Campos FO, Costa CM, Wilde AAM, Prassl AJ, Neic A *et al.* Predicting arrhythmia recurrence following catheter ablation for ventricular tachycardia using late gadolinium enhancement magnetic resonance imaging: implications of varying scar ranges. *Heart Rhythm* 2022;**19**:1604–10.
45. Laan D, Hopman L, Figueras IVRM, Sore B, Allaart CP, Kemme MJB *et al.* Ventricular tachycardia substrate mapping with cardiac computed tomography and cardiac magnetic resonance imaging: head-to-head comparison of two clinically available postprocessing platforms. *Heart Rhythm* 2025:S1547-5271(25)02921-2. doi:10.1016/j.hrthm.2025.09.028. Epub ahead of print.
46. Vullaganti S, Levine J, Raiker N, Syed AA, Collins JD, Carr JC *et al.* Fibrosis in hypertrophic cardiomyopathy patients with and without sarcomere gene mutations. *Heart Lung Circ* 2021;**30**:1496–501.